Sensors and Actuators A 165 (2011) 66–72

Contents lists available at ScienceDirect

Sensors and Actuators A: Physical

journal homepage: www.elsevier.com/locate/sna

Exploitation of aeroelastic effects for drift reduction, in an all-polymer air flow sensor

C. Song[a], A.R. Aiyar[b], S.-H. Kim[a,*], M.G. Allen[a,b]

[a] School of Electrical and Computer Engineering, Georgia Institute of Technology, 791 Atlantic Dr. NW, Atlanta, GA 30332, USA
[b] School of Chemical and Biomolecular Engineering, Georgia Institute of Technology, Atlanta, GA, USA

ARTICLE INFO

Article history:
Available online 13 January 2010

Keywords:
Vibration amplitude measurement
All-polymer air flow sensor
Flow-induced vibration
Drift reduction
Flex-PCB

ABSTRACT

This paper presents a vibration amplitude measurement method that greatly reduces the effects of baseline resistance drift in an all-polymer piezoresistive flow sensor or microtuft. The sensor fabrication is based on flexible printed circuit board (flex-PCB) technology to enable the potential for low-cost and scalable manufacture. Drift reduction is accomplished by discriminating the flow-induced vibration (‘*flutter*’) amplitude of the microtuft-based sensor as a function of flow velocity. Flutter peak-to-peak amplitude is measured using a microcontroller-based custom readout circuit. The fabricated sensor with the readout circuitry demonstrated a drift error of 2.8 mV/h, which corresponds to a flow-referenced drift error of 0.2 m/s of wind velocity per hour. The sensor has a sensitivity of 14.5 mV/(m/s) with less than 1% nonlinearity over the velocity range of 5–16 m/s. The proposed vibration amplitude measurement method is also applied to a sensor array with a modified structure and a reduced dimension, which demonstrated a sensitivity of 13.2 mV/(m/s) with a flow-referenced drift error of 0.03 m/s of wind velocity per hour.

1. Introduction

Flow sensors are of great interest to applications such as process control, metrology [1] and flight control involving unmanned aerial vehicles (UAVs) [2]. Among different types of flow sensors, bio-mimetic flow sensors mimicking fish hairs and cricket filiform hairs are the subject of much research. Typically, the nature-inspired bio-mimetic flow sensor has a three-dimensional (3D) out-of-plane cantilever with a sensing element to detect the air flow around it. Advances in microelectronics and micromachining technologies enable the fabrication of MEMS bio-mimetic flow sensors with good performance, based on silicon and/or polymer micromachining technologies. A bio-mimetic silicon-based capacitive flow sensor array with high-aspect ratio SU-8 microtufts was recently reported and demonstrated sensitivities of the order of 1 mm/s [3]. A silicon-based piezoresistive air flow sensor with SU-8 cilia has also been reported [4]. Although these approaches demonstrate good sensitivity, they require relatively complex fabrication sequences. Further, being silicon-based, it is challenging to cover large areas of vehicle wings with these flow sensors in a cost-effective manner. Polymer-based devices may overcome these challenges, at the expense of specific performance, and further exhibit good flexibility and scalability. These features are extremely important in applications requiring distributed sensor arrays in large and uneven surfaces such as UAV applications [2]. We have already demonstrated a 3D out-of-plane micromachined flexible piezoresistive all-polymer flow sensor array based on low-cost flexible-PCB technologies [5]. The piezoresistive all-polymer sensor provided a large resistance change without complex sensing circuitry for compensation and amplification of the sensor output. However, a significant resistance drift in the sensor output was observed [5], potentially limiting the applicability of the sensor.

In this paper, we propose a reduced-drift sensor measurement method that exploits aeroelastic ‘*flutter*’ effects [6,7] and demonstrate its application to a flex-PCB-based all-polymer flow sensor. The sensor comprises a 3D out-of-plane polymer cantilever member that can protrude into an embedding flow, and a piezoresistive readout element in the polymer member. Positioning the flexible polymer sensor in a flow results in a static deflection of the sensor, as well as a vibratory sensor flutter caused by aeroelastic effects. The amplitude of the flutter depends on the surrounding flow velocity and is empirically characterized. Microcontroller-based circuitry is used to extract the peak-to-peak vibration amplitude from the sensor output. Since the sensor output is now primarily dependent on the vibration-induced resistance change, as opposed to static deflection, the sensor output is relatively insensitive to DC resistance drift.

* Corresponding author. Tel.: +1 404 894 8807; fax: +1 404 894 2776.
E-mail address: seonghyok.kim@gmail.com (S.-H. Kim).

0924-4247/$ – see front matter
doi:10.1016/j.sna.2010.01.008

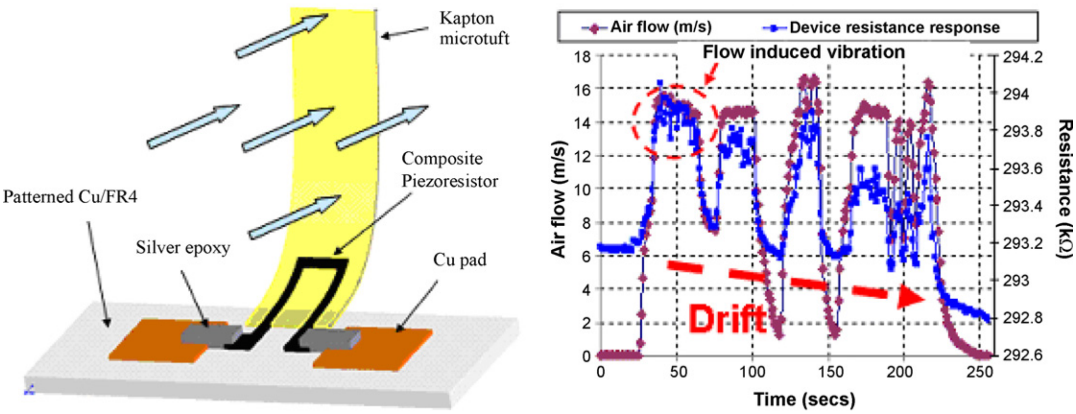

Fig. 1. Flex-PCB-based bio-mimetic air flow sensor and sensor output [5].

2. Principle of flow-induced vibration and its application to all-polymer flow sensor

Fig. 1 shows an all polymer flow sensor and its output response to air flows, previously reported by our research group [5]. The sensor comprises a 3D out-of-plane Kapton microtuft (length: 1.5 mm, width: 0.4 mm, thickness: 7.6 μm) and a carbon-black-loaded polydimethylsiloxane (PDMS) piezoresistor. Air flow across the microtuft causes deformation of the microtuft. The deformation, which is proportional to the distributed force on the microtuft, in turn, induces the strain in the piezoresistor [8]. The resistance of the piezoresistor therefore changes as a function of the strain induced by the applied wind velocity [8]. The relation between the resistance change and the strain is given by:

$$\frac{\Delta R}{R} = G\varepsilon,$$

where G (around 7.3) is the gauge factor of the piezoresistor, and ε is the strain in the piezoresistor [5].

We demonstrated the scalability and flexibility of the all-polymer flow sensor array, while addressing the sensor output resistance drift. This drift may be caused by various factors, including temperature variations and material property changes in elastomeric piezoresistive materials [5,9,10]. However, by closely observing the sensor output response, a fluctuating resistance is seen. This fluctuation is caused by flow-induced vibration of the cantilever beam, i.e., a '*fluttering*' or '*galloping*' effect, which refers to self-excited vibration of a bluff object induced by aerodynamic lift and drag forces [6,11,12]. The self-excited vibration is a result of negative damping due to aerodynamic lift forces acting in the direction of the motion of the bluff object [11,12]. Theoretically, the vibration amplitude of the fluctuation is proportional to the wind velocity [12]. In order to verify this phenomenon, the resistance change in the previously reported all-polymer flow sensor is empirically characterized with varying wind velocity using a digital multimeter (Keithley). In order to facilitate the vibration of the microtuft [6], the sensor which is used for the evaluation has a longer cantilever-like microtuft, which measures 3.5 mm long, 0.6 mm wide and 7.6 μm thick. As shown in Fig. 2, the amplitude of the vibration-induced resistance increases as the wind velocity increases. This confirms the validity of the proposed vibration amplitude measurement method.

Based on this observation, the sensor readout scheme of Fig. 3 is proposed. As shown in Fig. 3, the amplitude of changes in the vibration-induced resistance increases when the wind velocity becomes larger, independent of the absolute value of resistance. Therefore, the baseline drift can be reduced by filtering out low frequency signals from the sensor output, followed by signal pro-

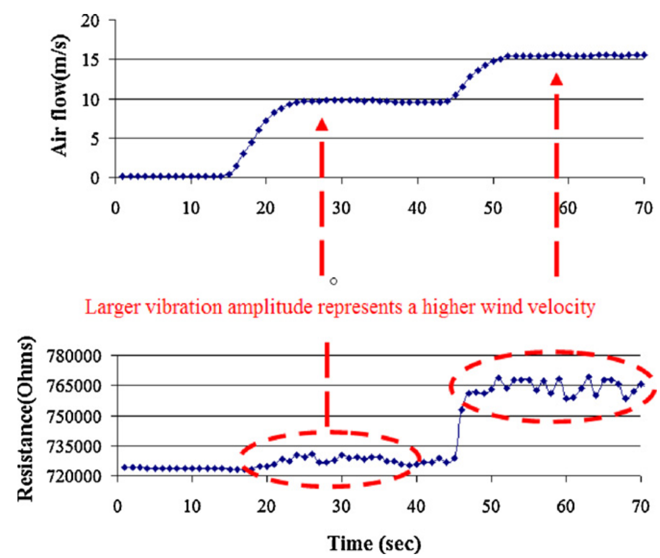

Fig. 2. Sensor output of the polymer-based flow sensor using direct resistance measurement with different wind velocities applied: wind velocity profile (upper) and sensor output (lower). Note that the vibration amplitude increases as the wind velocity increases.

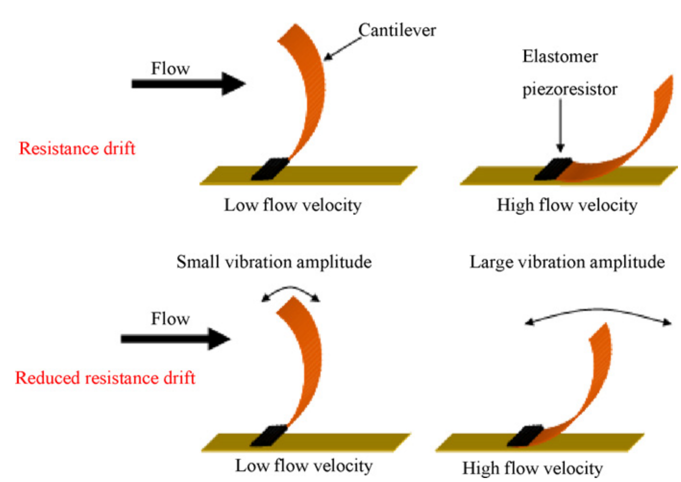

Fig. 3. (Top) Conventional piezoresistive-based airflow sensor. (Bottom) Concept of the proposed vibration amplitude measurement method using flow-induced vibration.

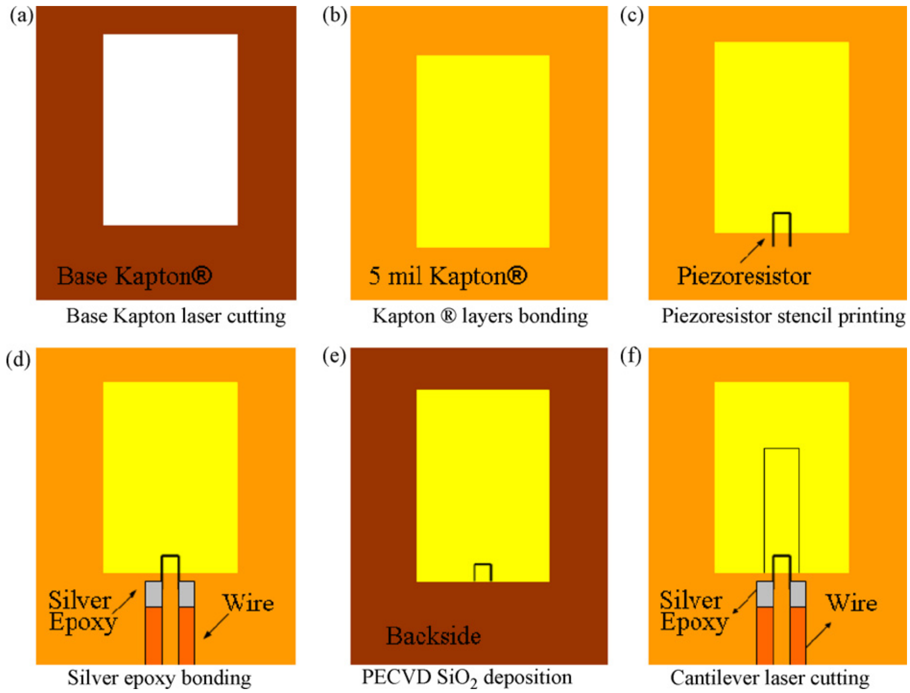

Fig. 4. Fabrication process sequence. (a) Base Kapton laser cutting, (b) Kapton® layers bonding, (c) piezoresistor stencil printing, (d) silver epoxy bonding, (e) PECVD SiO_2 deposition and (e) cantilever laser cutting.

cessing for peak-to-peak amplitude calculation. It is assumed that baseline drift is slow compared to the time scale of the flow-induced sensor vibration.

3. Fabrication process for all-polymer flow sensor

The all-polymer flow sensor used in the experiment is fabricated using the previously reported flexible-PCB-based process [5], incorporating laser-micromached Kapton® (Dupont) and a stencil-printed piezoresistive elastomer (Elastosil® LR3162, Wacker Chemie AG). A 125 μm thick Kapton film is laser machined using a CO_2 laser (Gravograph Newhermes) and laminated with a 7.6 μm thick Kapton film to form the base and device layers, respectively (Fig. 4(a) and (b)). A piezoresistor is then stencil-printed on the device Kapton layer and cured at 130 °C for 2 h (Fig. 4(c)). Interconnections between the piezoresistor and the external circuitry are achieved using silver epoxy (Fig. 4(d)), followed by plasma enhanced chemical vapor deposition (PECVD) of SiO_2 on the opposite side of the piezoresistor (Fig. 4(e)). This deposition will cause an out-of-plane deflection due to stress gradients induced by the silicon dioxide film upon release of the microtuft. The deposition is followed by excimer laser (248 nm, Lambda Physik) cutting of the in-plane cantilevers to release the microtuft (Fig. 4(f)).

Fig. 5 shows a fabricated all-polymer piezoresistive flow sensor. The cantilever-like microtuft is 3.5 mm long, 0.6 mm wide and 8.2 μm thick. The elastomeric piezoresistor is 110 μm wide, 1.9 mm long, and has an average thickness of 13 μm. The measured resistance of the piezoresistor in its initial curved state is approximately 700 kΩ.

4. Sensor readout circuit

A block diagram of the sensor readout circuit for the vibration amplitude measurement of the all-polymer flow sensor is shown in Fig. 6. The piezoresistor in the flow sensor is connected to a single-element-varying, voltage-driven Wheatstone bridge, which is composed of three 700 kΩ non-variable resistors and the piezoresistive sensor as the varying element. The output of the bridge is fed to an instrumentation amplifier (INA122, Texas Instruments) with a gain of 6. When there is a resistance variation ΔR in the piezoresistor with an initial resistance of R_o, the output of the instrumentation amplifier is given by:

$$V_o = \frac{1}{2}V_s\left(\frac{\Delta R}{2R_o + \Delta R}\right)G \approx \frac{1}{4}V_s\left(\frac{\Delta R}{R_o}\right)G,$$

where V_s is the supply voltage of the bridge and G is the gain of the amplifier.

In order to extract the peak-to-peak vibration amplitude of the sensor output and convert the resistive output to a voltage output, a microcontroller (MSP430F2012, Texas Instruments) with built-in 10-bit successive approximation (SAR) analog-to-digital converter

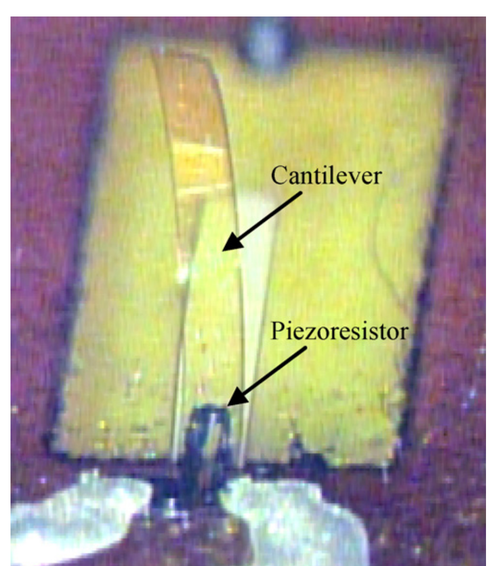

Fig. 5. Fabricated all-polymer flow sensor.

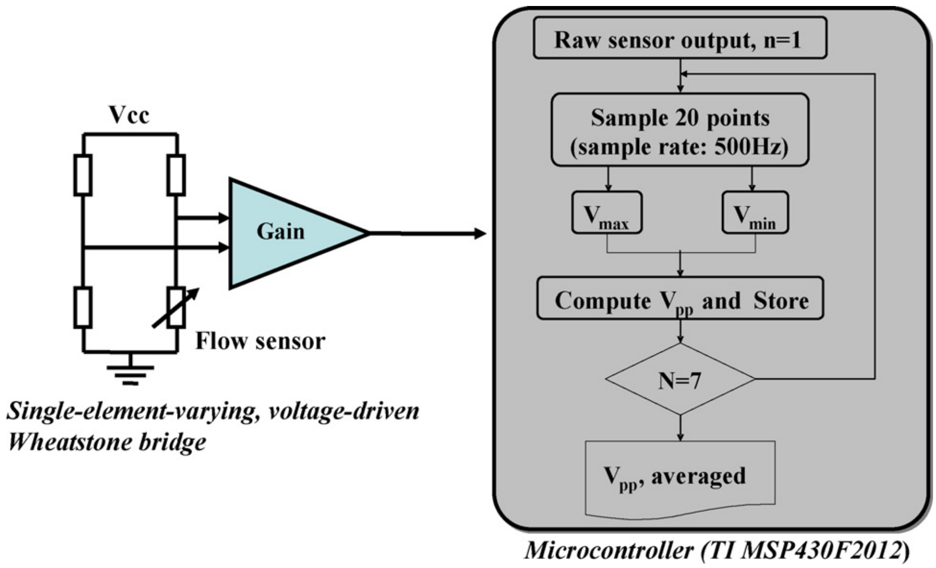

Fig. 6. Schematic illustration of sensor readout circuit and implementation of vibration amplitude measurement method.

(ADC) is used for data acquisition and signal processing. A light-emitting-diode (LED) is optionally connected to demonstrate real-time visualization of the measured wind velocity.

The resonant frequency of the sensor is estimated using the following formula:

$$f = \frac{3.52}{2\pi}\sqrt{\frac{EI}{u_1 l^4}},$$

where E is the Young's modulus of the Kapton film, I is the moment of inertia, u_1 is the product of the density of the Kapton film and the cross-sectional area of the microtuft [11]. The estimated resonant frequency is around 130 Hz. Therefore, the microcontroller's 500 Hz sampling rate is adequate to fully capture the vibration information. The microcontroller samples the amplifier output at *the configured* sampling rate and stores 20 sampled data points in its internal memory. The peak-to-peak vibration amplitude of the output voltage is derived from this data set by determining the difference between the maximum and minimum values in the stored data. Seven of these peak-to-peak measurements are then averaged to produce the final output of the sensor read-out circuitry, which indicates the flow-induced vibration amplitude.

5. Wind tunnel testing

A fabricated all-polymer flow sensor with the readout circuitry is tested in a bench top wind tunnel (ST 180 Scantek 2000), as shown in Fig. 7. A thermal anemometer (Omega FMA-605-I) with a measurement range of 0–25 m/s is used as a reference sensor for measuring the mean free stream wind velocity. The fabricated all-polymer flow sensor is connected to the above-described readout circuitry.

Fig. 8 shows the sensor output response after the readout circuitry and the reference sensor output as the air flow is repetitively cycled between 0 m/s and 12 m/s. The results show that the baseline drift which is observed in conventional direct measurement method, shown in Fig. 1, has been greatly reduced. The maximum value of the sensor output is 225 mV when the wind velocity is 12 m/s. Although the sensor exhibits a threshold behavior and is sensitive to velocities only in the range of 5–12 m/s, this range is adjustable by changing the geometry of the sensor. The sensor is also tested without applying wind velocity to characterize the zero-input drift as shown in Fig. 9. The standard deviation of the sensor output from 1-h data acquisition is 2.8 mV, which corresponds to a flow-referenced drift error of 0.2 m/s wind velocity per hour.

Fig. 10 shows the measured vibration amplitude of the all-polymer flow sensor when the wind velocity varies between

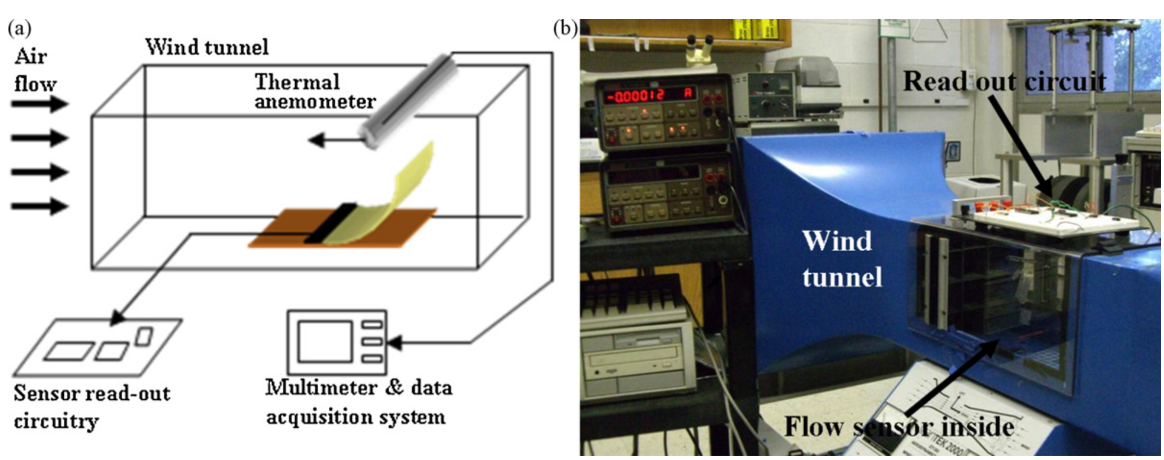

Fig. 7. (a) Schematic illustration of sensor testing and (b) wind tunnel experimental setup.

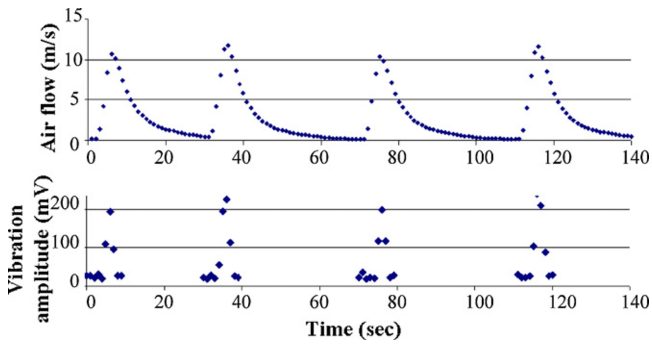

Fig. 8. Output of the all-polymer flow sensor from the proposed vibration amplitude measurement method: reference wind velocity (upper) and the measured sensor response (lower).

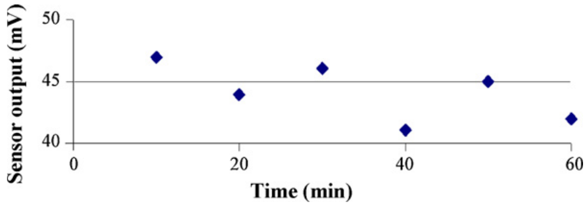

Fig. 9. Zero-input drift of the all-polymer flow sensor as a function of time using the reduced-drift measurement approach.

0 m/s and 16 m/s. With an amplifier gain of 6 and a Wheatstone driving voltage of 5.12 V, the sensitivity of the sensor measures 14.5 mV/(m/s), with non-linearity of 1% over the range of 5–16 m/s wind velocity. This result demonstrates that the vibration amplitude is proportional to the wind velocity, which is in accordance with the theoretical background discussed earlier in this paper. As can be seen in Figs. 8 and 10, the all-polymer flow sensor output exhibits variation across data points with nearly identical reference sensor readings. Sources of this measurement inconsistency might include reference sensor drift, variation in the Wheatstone bridge supply voltage, microcontroller measurement errors, and the extremely large baseline drift of the all-polymer air flow sensor.

6. Improvement of sensor performance

In most air flow sensor applications, especially in flight control applications involving unmanned aerial vehicles, smaller air flow sensors are preferred in order for minimal obstruction of the air flow without degrading the sensor performance. In this work, after a modification of the sensor structure was performed, an all-polymer air flow sensor with reduced dimension as well as a higher sensitivity when vibration amplitude measurement method is applied was fabricated. A 3×3 sensor array with all-polymer flow sensors with modified geometry is fabricated as shown in Fig. 11. The fabricated all-polymer piezoresistive flow sensor array has microtufts which are composed of two cantilevers with 0.7 mm in length and 50 μm in width and a 1.1 mm wide and 0.4 mm long flapper at the end. The elastomeric piezoresistor is evenly coated on both cantilevers and the flapper with an average thickness of 16 μm. The measured resistance of the piezoresistor in its initial curved state is approximately 370 kΩ.

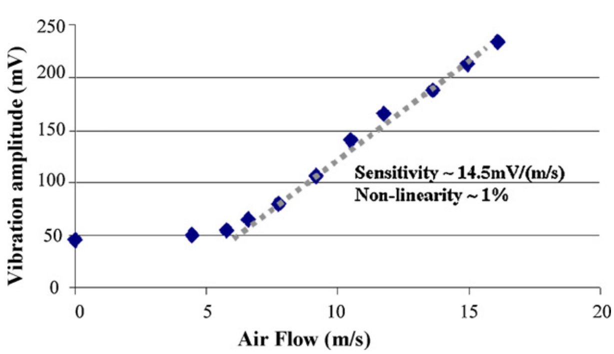

Fig. 10. Sensor output as a function of the wind velocity, acquired by the vibration amplitude measurement method.

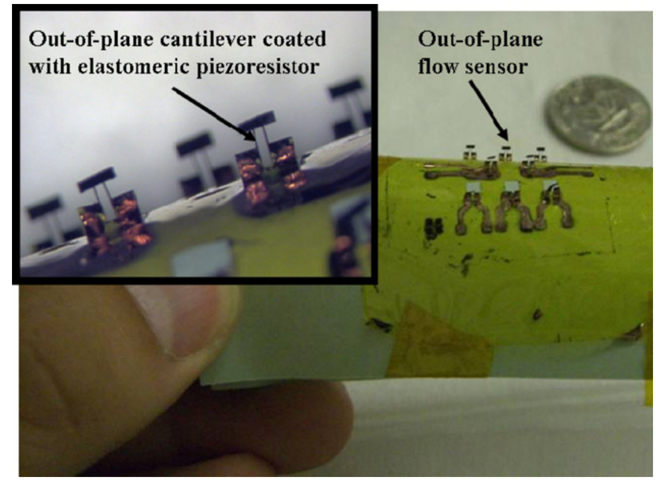

Fig. 11. Fabricated all-polymer air flow sensor array with a modified geometry.

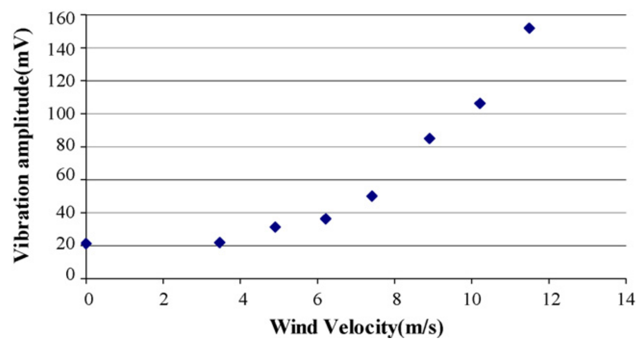

Fig. 12. Sensor output as a function of the wind velocity, acquired by the vibration amplitude measurement method.

Fig. 12 shows the measured output of the fabricated all-polymer flow sensor array using the proposed vibration amplitude measurement. The wind velocity varies between 0 m/s and 12 m/s. With an amplifier gain of 5 and a Wheatstone driving voltage of 3.33 V,

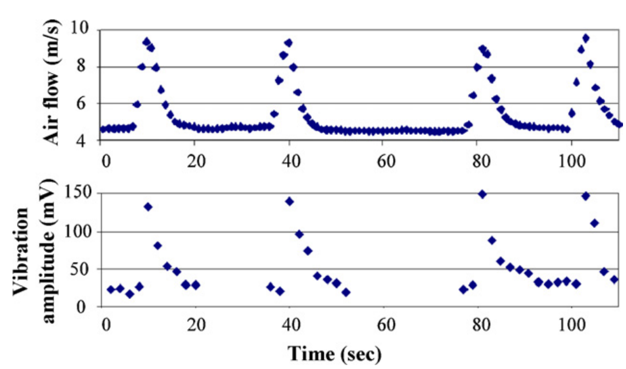

Fig. 13. Output of the all-polymer flow sensor from the proposed vibration amplitude measurement method: reference wind velocity (upper) and the measured sensor response (lower).

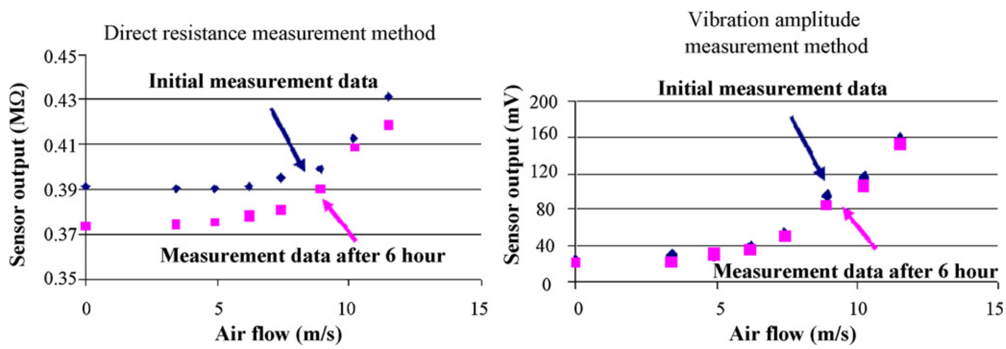

Fig. 14. Long term drift comparison between direct resistance measurement method and vibration amplitude measurement method. Blue dots: initial measurement data. Purple dots: measurement data after 6 h. Experiments are done using an all-polymer air flow sensor with optimized geometry. (For interpretation of the references to color in this figure legend, the reader is referred to the web version of the article.)

Table 1
Performance characteristics of a typical microtuft-based flow sensor.

	Original geometry	Modified geometry
Device dimension	Single cantilever: 3.5 mm (l) × 0.6 mm (w)	Dual cantilevers: 0.7 mm (l) × 50 μm (w) Flapper: 0.4 mm (l) × 1.1 mm (w)
Sensitivity	14.5 mV/(m/s) @ 5.12 V gain 6	13.2 mV/(m/s) @ 3.33 V gain 5
Threshold	~5 m/s	~4 m/s
Non-linearity	1% (5–12 m/s)	4.7% (4–12 m/s)
Zero-input drift	0.2 m/s in 1 h	0.033 m/s in 1 h

the sensitivity is measured to be 13.2 mV/(m/s). This measured sensitivity is equivalent to a sensitivity of 24.4 mV/(m/s) with an amplifier gain of 6 and a Wheatstone driving voltage of 5.12 V, a 68% of sensitivity improvement compared with a 14.5 mV/(m/s) sensitivity of aforementioned sensor. In addition, this improved sensitivity results in a threshold drop from 5 m/s to 4 m/s as shown in Fig. 12. Fig. 13 shows the fabricated sensor output response and the reference sensor output when the air flow is repetitively cycled between 4 m/s and 10 m/s. The sensor has demonstrated reduced baseline drift as well as improved minimum air-flow velocity detection.

7. Comparison between direct resistance measurement method and proposed vibration amplitude measurement method

In order to verify the improved characteristics of the proposed vibration amplitude measurement method, the fabricated sensor output is measured using both direct resistance measurement method and the proposed method. Then the outputs were compared as shown in Fig. 14. The sensor is measured twice with 6-h intervals between measurements. Both during measurements and in between measurements, the all-polymer air flow sensor was kept without any environmental conditioning such as humidity control, temperature control, or air filtering. Blue dots represent the initial measurement data and the purple dots represent the measurement data after 6 h. With the direct resistance measurement method, the baseline resistance drift was clearly observed. However, in the experimental results using the vibration measurement method, the blue and purple dots almost fully overlap, which indicates that the drift is significantly reduced. Velocity-referenced baseline drift using the vibration amplitude measurement method was 0.033 (m/s)/h.

8. Conclusion

This paper proposes a peak-to-peak vibration amplitude measurement method for wind velocity sensing as a baseline resistance drift-reduction method. The proposed method exploits aeroelastic flutter-based flow-induced vibration and has been validated by the wind tunnel test of a flexible-PCB-based all-polymer piezoresistive air flow sensor. The measured characteristics demonstrate a significant reduction of output drift using the proposed measurement method, when compared to that of the conventional direct measurement method. In addition, sensors with different geometries were tested with the proposed measurement method as shown in Table 1. The proposed measurement method is promising since it significantly reduces the drift caused by the intrinsic property of the materials as well as environmental changes.

Acknowledgements

This work was supported in part by the U.S. Air Force under the Multidisciplinary University Research Initiative under contract number FA9550-05-1-0411. The authors would like to thank Prof. Ari Glezer for valuable discussion.

References

[1] G.R. Hendrey, D.S. Ellsworth, K.F. Levin, J. Nagy, A free-air enrichment system for exposing tall forest vegetation to elevated atmospheric CO_2, Glob. Change Biol. 5 (1999) 293–309.
[2] R. Zhu, P. Liu, X.D. Liu, F.X. Zhang, Z.Y. Zhou, A low-cost flexible hot-film sensor system for flow sensing and its application to aircraft, in: Digest Tech. Papers IEEE MEMS'09 Conference, Sorrento, January 25–29, 2009, pp. 527–530.
[3] C.M. Bruinink, R.K. Jaganatharaja, M.J. de Boer, E. Berenschot, M.L. Kolster, T.S.J. Lammerink, R.J. Wiegerink, G.J.M. Krijnen, Advancements in technology and design of biomimetic flow-sensor arrays, in: Digest Tech. Papers IEEE MEMS'09 Conference, Sorrento, January 25–29, 2009, pp. 152–155.
[4] N. Chen, C. Tucker, J.M. Engel, Y. Yang, S. Pandya, C. Liu, Design and characterization of artificial haircell sensor for flow sensing with ultrahigh velocity and angular sensitivity, J. Microelectro-mech. Syst. 16 (2007) 999–1014.
[5] A.R. Aiyar, C. Song, S.H. Kim, M.G. Allen, An all polymer air-flow sensor array using a piezoresistive composite elastomer, Smart Mater. Struct. 18 (2009) 115002.
[6] R.D. Blevins, Flow-induced Vibration, Van Nostrand Reinhold Company, New York, 1977.
[7] K.H. Kim, Y.H. Seo, Self-resonant flow sensor using resonance frequency shift by flow-induced vibration, in: Digest Tech. Papers IEEE MEMS'09 Conference, Sorrento, January 25–29, 2009, pp. 511–514.
[8] Y.H. Wang, C.Y. Lee, C.M. Chiang, A MEMS-based air flow sensor with a free-standing micro-cantilever structure, IEEE Sensors J. 7 (2007) 2389–2401.
[9] J.M. Engel, J. Chen, C. Liu, D. Bullen, Polyurethane rubber all-polymer artificial hair cell sensor, J. Microelectro-mech. Syst. 15 (2006) 729–736.

[10] E.P. Scilingo, F. Lorussi, A. Mazzoldi, D.D. Rossi, Strain-sensing fabrics for wearable kinaesthetic-like systems, IEEE Sensors J. 3 (2003) 460–467.
[11] J.P. Den Hartog, Mechanical Vibrations, McGraw-Hill Book Company, New York, 1956.
[12] V. Mukhopadhyay, J. Dugundji, Wind excited vibration of a square section cantilever beam in smooth flow, J. Sound Vib. 45 (1976) 329–339.

Biographies

Chao Song was born in Shanghai, China, in 1982. He received his B.S. degree in electrical engineering from Shanghai Jiaotong University in 2004. In 2007, he obtained his Dipl.-Ing in electronics and signal processing and his M.S. degree in microelectronics circuits and microsystems from ENSEEIHT, Toulouse, France. In 2008, he received his M.S. degree in electrical and computer engineering from Georgia Institute of Technology and started working towards his Ph.D. degree in the research group of Professor Mark G. Allen. His current research interests include MEMS flow sensors and sensor interface circuits.

Avishek Aiyar joined the Georgia Institute of Technology (Atlanta, GA) in 2005 as a graduate research assistant, where he worked in the research group of Prof. M.G. Allen, after earning a B.S. degree in chemical engineering from India (2005). His interests focused on developing new microfabrication techniques for miniaturized all polymer flow sensors, based on which he graduated with an M.S. (2008) degree in chemical engineering. His currents interests are in the area of polymeric semiconductors, and he is presently working towards a Ph.D. thesis on organic field effect transistors.

Seong-Hyok Kim received the B.S.E., M.S. degree at the Department of Electrical Engineering, Seoul National University in 1996, 1998, respectively, and the Ph.D. degree in electrical engineering and computer science from Seoul National University in 2002. His doctorate research focused on the design and the fabrication of a silicon microgyroscope operating at atmospheric pressure. After joining LG Electronics Institute of Technology as a Senior Research Engineer in 2002, he participated in the design and fabrication of a wide variety of microelectromechanical systems (MEMS) devices for portable electronics. Dr. Kim joined Georgia Institute of Technology as a postdoctoral fellow in 2005 and became a Research Engineer II at Micro Sensors and Micro Actuators Laboratory (MSMA Lab.) in 2007. Dr. Kim has published more than 43 peer-reviewed journal and conference articles and holds 29 Korean/International patents in the field of MEMS including power MEMS, bio MEMS, optical MEMS, and MEMS sensors and actuators. His current research interests include 3D micro/nanostructures for integrated power electronics, energy storing devices and miniaturized energy harvester, polymeric microneedle/micro-electrode-array (MEA) for human health and environmental monitoring, flexible-PCB-based sensors for robotics, and micro/nanofabrication processes for micro/nanoinstruments.

Mark G. Allen (M'89–SM'04) received the B.A. degree in chemistry, the B.S.E. degree in chemical engineering, and the B.S.E. degree in electrical engineering from the University of Pennsylvania, Philadelphia, and the S.M. and Ph.D. degrees from the Massachusetts Institute of Technology, Boston. Since 1989, he has been with the faculty of the School of Electrical and Computer Engineering, Georgia Institute of Technology, Atlanta, where he currently holds the rank of Regents' Professor and the J.M. Pettit Professorship in microelectronics, as well as a joint appointment with the School of Chemical and Biomolecular Engineering. He also holds the position of Senior Vice Provost for Research and Innovation, and is charged with overseeing Georgia Tech's interdisciplinary research centers, managing Georgia Tech's sponsored research portfolio, and guiding the commercialization of Georgia Tech research results and intellectual property. He is the Editor-in-Chief of the *Journal of Micromechanics and Microengineering*. His current research interests are in the field of microfabrication and nanofabrication technology, with emphasis on new approaches to fabricate devices with characteristic lengths in the micro- to nanoscale from both silicon and nonsilicon materials. Examples include micromagnetics, high-temperature sensors, small-scale power generation, biofluidic microvasculatures and implantable microsensors, and the use of microstructures to create nanostructures. Dr. Allen was the Co-Chair of the 1996 IEEE/ASME Microelectromechanical Systems Conference.